16th World Conference on Earthquake, 16WCEE 2017

Santiago Chile, January 9th to 13th 2017

Paper N° 1480 (Abstract ID)

Registration Code: S-R1461752962

HYSTERETIC BEHAVIOR OF HIGH-DAMPING RUBBERS UNDER NON-PROPORTIONAL PLANE LOADING

SJ. Wang[(1)], WC. Lin[(2)], JS. Hwang[(3)], BW. Huang[(4)]

[(1)] *Research Fellow, National Centre for Research on Earthquake Engineering, sjwang@ncree.narl.org.tw*
[(2)] *Assistant Researcher, National Centre for Research on Earthquake Engineering, wclin@ncree.narl.org.tw*
[(3)] *Professor, National Taiwan University of Science and Technology,JSH@mail.ntust.edu.tw*
[(3)] *Graduate Student, National Taiwan University of Science and Technology,m10105329@mail.ntust.edu.tw*

Abstract

High-damping rubber (HDR) bearings have gradually become a commonly used type of seismic isolators worldwide. Because of the complex material compound, their actual hysteretic behavior is highly nonlinear and may not be very well represented by the existing bilinear approximation. In this study, first, a modified mathematical model is proposed for comprehensively characterizing the unilateral hysteretic behavior of HDR bearings under sinusoidal and triangular reversal loading. In addition to unilateral reversal loading tests, HDR bearings are tested with different non-proportional plane loading patterns, including circular and figure-eight orbits. It is found that under bilateral loading, the torsional coupling effect is significant on the mechanical properties and hysteretic behavior of HDR bearings. Therefore, integrating the three-dimensional constitute law and the plane vector concept with the modified unilateral model, a further extended mathematical model for HDR bearings under non-proportional plane loading is developed. The accuracy and applicability of the modified and further extended mathematical models are verified through comparison with the test results.

Keywords: high-damping rubber bearing; multiaxial hysteretic behavior; non-proportional plane loading; mathematical model; torsional coupling effect

1. Introduction

Although the bilinear approximation may not very well represent the highly nonlinear hysteretic behavior of HDR bearings, it is still commonly adopted in current practical isolation design as long as the design result can be guaranteed on safe side. A few sophisticated models which are capable of more accurately characterizing the hysteretic behavior of High-damping rubber (HDR) bearings have been provided in past researches. However, their complexity more or less impedes the implementation into most commercial computation tools.

A simple mathematical model accounting for the unilateral shear force experienced by HDR bearings as a combination of restoring force and damping force was proposed and experimentally verified by Hwang et al. [1]. To further predict the multiaxial hysteretic behavior of laminated rubber bearings, Abe et al. [2, 3] derived a two-dimensional model on the basis of the Özdemir model [4] and the three-dimensional constitutive law. It was also experimentally demonstrated that the hysteretic behavior of HDR bearings under bilateral loading can be well simulated by the model.

In this study, a scaled-down HDR bearing is tested with different loading patterns, including unilateral reversal loading and non-proportional plane loading. Accordingly, two mathematical models modified from Hwang's and Abe's analytical models respectively accounting for the hysteretic behavior of HDR bearings under unilateral and bilateral loading are developed. The accuracy and applicability of the two modified models are verified through comparison with a series of test results. In addition, the torsional coupling effect on the mechanical properties and hysteretic behavior of HDR bearings is experimentally discussed.

2. Mathematical Model by Hwang et al.

In the mathematical model proposed by Hwang et al. [1], the shear force experienced by an elastomeric bearing was characterized in the form of

$$F\left(x(t),\dot{x}(t)\right)=K\left(x(t),\dot{x}(t)\right)x(t)+C\left(x(t),\dot{x}(t)\right)\dot{x}(t) \tag{1}$$

where $x(t)$ and $\dot{x}(t)$ are the relative displacement and relative velocity of the elastomeric bearing at time *t*, respectively. The stiffness and damping coefficient at time *t* are respectively given by

$$K\left(x(t),\dot{x}(t)\right)=a_1+a_2x^2(t)+a_3x^4(t)+\frac{a_4\exp\left[a_9\int_0^t F\left(x(t),\dot{x}(t)\right)dx(t)\right]}{\cosh^2\left(a_5\dot{x}(t)\right)} \tag{2}$$

$$C\left(x(t),\dot{x}(t)\right)=\frac{a_6+a_7x^2(t)}{\sqrt{a_8^2+\dot{x}^2(t)}}\left\{1+\exp\left[a_{10}\int_0^t F\left(x(t),\dot{x}(t)\right)dx(t)\right]\right\} \tag{3}$$

where $a_1\sim a_{10}$ are to-be-determined coefficients from cyclic loading or dynamic tests by using the nonlinear-least squares method or downhill simplex method. The cyclic softening behavior of an elastomeric bearing can be regarded as a function of energy dissipation. Thus, the integral term $\int_0^t F\left(x(t),\dot{x}(t)\right)dx(t)$ together with the to-be-determined coefficients are applied in Eq. (2) and Eq. (3) to respectively describe the degradation of stiffness and the variation of hysteresis loop area.

3. Multiaxial Loading Testing

A scaled-down HDR bearing is schemed to be tested under unilateral reversal loading and non-proportional plane loading. The diameter of the HDR bearing specimen is 150mm. It comprises 25 layers of rubber with a

thickness of 1.97mm for each as well as 24 layers of steel shim with a thickness of 1.2mm for each. The test setup is illustrated in Fig.1. As observed from Fig.1, the vertical load on the bearing is exerted by an oil jack, while the lateral displacement is executed by two mutually orthogonal servo-control actuators connected with the moveable platen. A linear guide system is installed underneath the platen to reduce the friction force induced by the test system. An external load cell is installed to measure the actual force responses of the bearing during tests. The unilateral test protocols under triangular and sinusoidal reversal loading are respectively detailed in Tables 1 and 2, and the bilateral ones under non-proportional plane loading, including circular and figure-eight orbits, are detailed in Table 3. The equations of the plane loading paths shown in Fig.2 are given by

Circular orbit:

$$U_X = U_0 \sin \omega t \tag{4}$$

$$U_Y = U_0 \cos \omega t \tag{5}$$

Figure-eight orbit:

$$U_X = U_0 \sin \omega t \tag{6}$$

$$U_Y = U_0 \sin 2\omega t \tag{7}$$

where U_X and U_Y are the displacement components in two principal horizontal directions, i.e. X and Y directions, respectively; U_0 is the displacement amplitude; ω is the angular frequency.

Fig. 1 – Test installation

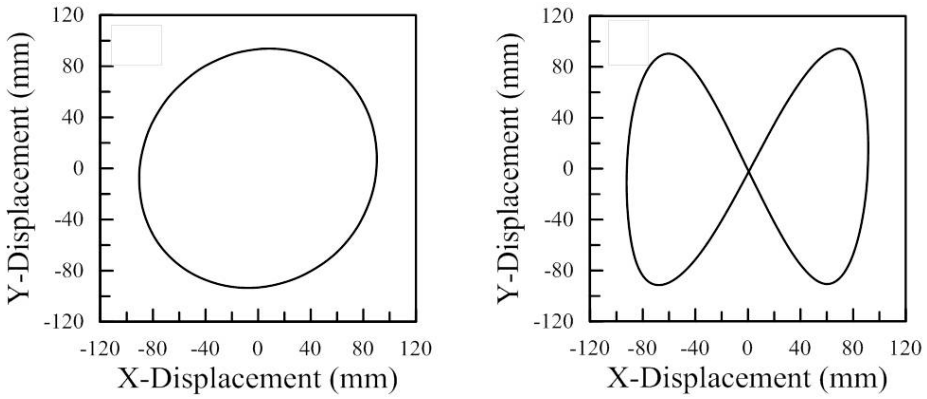

(a) circular orbit (b) figure-eight orbit

Fig. 2 – Plane loading paths

Table 1 – Unilateral test protocols under triangular reversal loading

Vertical Stress (kg/cm^2)	Horizontal Shear Strain (%)	Horizontal Displacement Amplitude (mm)	Horizontal Velocity (mm/sec)	Cycles
50	50	24.63	24.63 49.26 73.89	3
	100	49.25		
	150	73.88		
	200	98.50		
	250	123.13		

Table 2 – Unilateral test protocols under sinusoidal reversal loading

Vertical Stress (kg/cm^2)	Horizontal Shear Strain (%)	Horizontal Displacement Amplitude (mm)	Frequency (Hz)	Cycles
50	50	24.63	0.125 0.25	3
	100	49.25		
	150	73.88		
	200	98.50		
	250	123.13		

Table 3 – Bilateral test protocols under non-proportional plane loading

Orbit	Vertical Stress (kg/cm^2)	Horizontal Shear Strain (%)	Horizontal Displacement Amplitude (mm)	Frequency (Hz)	Cycles
Circular	50	50	24.63	0.0125 0.05 0.1 0.2	3
		100	49.25		
		150	73.88		
		200	98.50		
Figure-eight	50	50	24.63	0.0125 0.05 0.1 0.2	3
		100	49.25		
		150	73.88		
		200	98.50		

4. Modified Mathematical Model under Unilateral Reversal Loading

The comparison of unilateral test results and predictions by Hwang's analytical modal is shown in Fig.3. As observed from Fig.3(a), the prediction for the hysteretic behavior of HDR bearings under sinusoidal reversal loading has a good agreement with the test result. However, the prediction result is not acceptable when subjected to triangular reversal loading, as shown in Fig.3(b). It is because that not only the relative displacement

$x(t)$ but the relative velocity $\dot{x}(t)$ is the variable of the mathematical model given in Eq. (2) and Eq. (3). Under triangular reversal loading, the relative velocity history will become a typical step function, leading to a sudden force change at the transition of velocity directions. It implies that Hwang's analytical modal might be only appropriate for characterizing the unilateral hysteretic behavior of HDR bearing under harmonic loading.

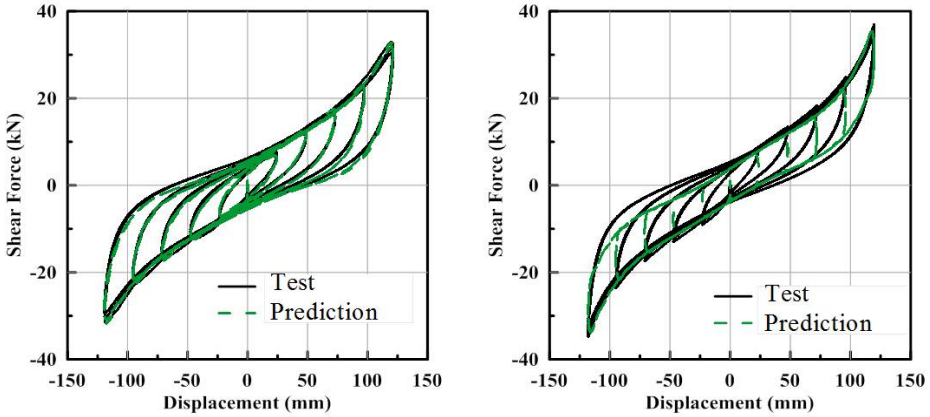

(a) sinusoidal reversal loading (b) triangle reversal loading

Fig. 3 – Experimental and predicted hysteretic behavior under different unilateral loading patterns (Hwang's modal)

The analytical models developed by both Hwang et al. and Abe et al. feature the hysteretic behavior of HDR bearings as a combination of restoring force and damping force. Therefore, referring to Hwang's and Abe's analytical models, a modified mathematical model for comprehensively characterizing the unilateral hysteretic behavior of HDR bearings is proposed herein.

$$F\left(x(t),\dot{x}(t)\right)=F_1(t)+F_2(t) \tag{8}$$

$$F_1(t)=\left[a_1+a_2x^2(t)+a_3x^4(t)\right]x(t) \tag{9}$$

$$\dot{F}_2(t)=\left[a_4+a_5x^2(t)\right]\left[\dot{x}(t)-\left|\dot{x}(t)\right|\left|\frac{F_2(t)}{Y_t}\right|^{a_6}\operatorname{sgn}\left(\frac{F_2(t)}{Y_t}\right)\right] \tag{10}$$

$$Y_t=a_7+\left[1+\left|\frac{x(t)}{a_8}\right|^{a_9}\right] \tag{11}$$

where the $F_1(t)$ is the nonlinear restoring force, which is similar to Eq. (2) multiplied by $x(t)$ but without considering the energy dissipation term related to $\dot{x}(t)$; $F_2(t)$ is the hysteresis force, which is simulated by the hysteretic behavior of an elastoplastic spring; Y_t represents the yielding force; $a_1 \sim a_9$ are to-be-determined coefficients from cyclic loading or dynamic tests.

Through comparison with the test results shown in Fig.4, the modified mathematical model indeed can well capture the unilateral hysteresis behavior of HDR bearings under both sinusoidal and triangular reversal loading.

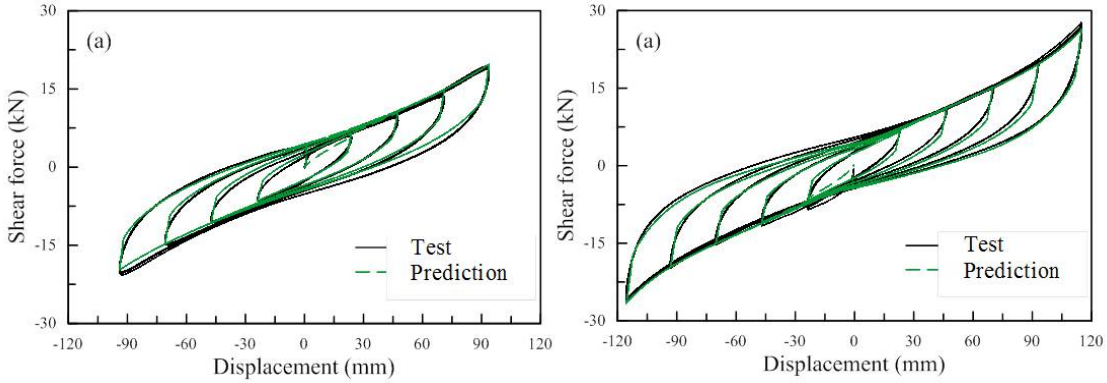

(a) sinusoidal reversal loading (b) triangle reversal loading

Fig. 4 – Experimental and predicted hysteresis behavior under different unilateral loading patterns (modified model)

4. Non-proportional Plane Loading Test Results and Further Extended Mathematical Model

Based on experimental observation, Yamamoto et al. [5] indicated that the torsional coupling effect plays a crucial role in the bilateral hysteresis behavior of HDR bearings. As observed from the comparison of X directional hysteresis loops under unilateral reversal loading and non-proportional plane loading shown in Fig.5, there exists a significant difference because of the torsional coupling effect, which results in the local shear strain increased. Besides, it is apparent that different plane loading patterns cause diverse torsional coupling extents.

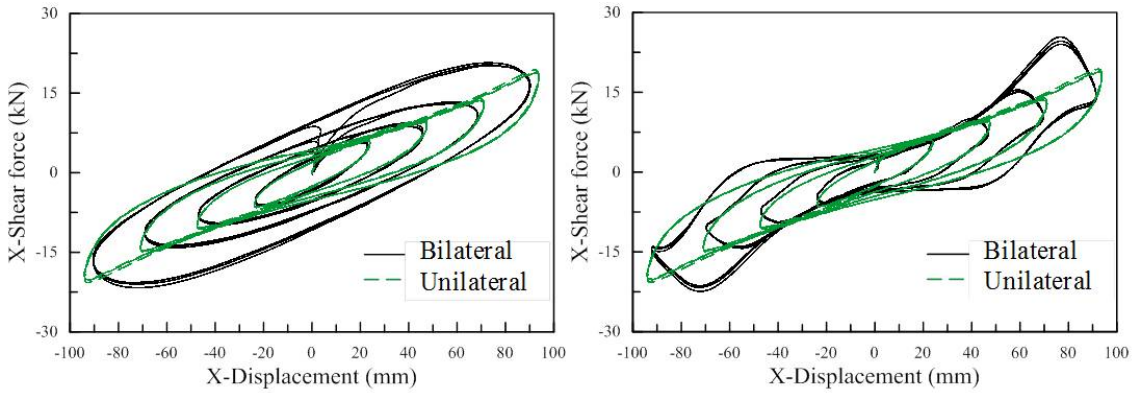

(a) circular orbit (b) figure-eight orbit

Fig. 5 – X directional hysteresis loops under unilateral and bilateral loading

The comparison of X directional effective shear modulus and equivalent damping ratio under unilateral reversal loading and non-proportional plane loading with the same shear strain level is shown in Fig.6. It is found that the calculated effective shear modulus under unilateral loading is the largest, while that under figure-eight orbit loading is the smallest. In addition, the calculated equivalent damping ratio under circular orbit loading is the largest, while that under unilateral loading is the smallest.

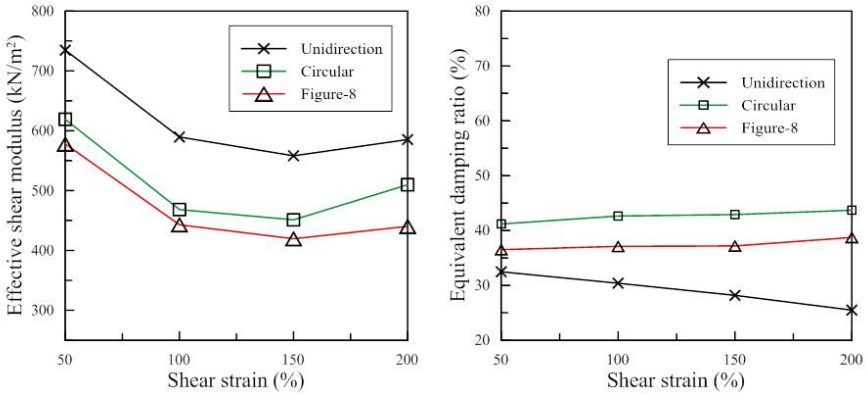

Fig. 6 – X directional properties under unilateral and bilateral loading

Referring to the modified model, a further extended mathematical model for characterizing the bilateral hysteresis behavior of HDR bearings is proposed herein.

$$\vec{F} = \begin{Bmatrix} F_x \\ F_y \end{Bmatrix} = \vec{F}_1 + \vec{F}_2 \tag{12}$$

where F_X and F_Y are the force components in two principal horizontal directions, i.e. X and Y directions, respectively.

Based on the plane vector concept, the relative displacement, relative velocity, and shear force in two principal horizontal directions, X and Y directions, can be expressed in the form of vectors herein.

$$\vec{U} = \begin{Bmatrix} U_x & U_y \end{Bmatrix}^T, \left|\vec{U}\right| = \sqrt{U_x^2 + U_y^2} \tag{13}$$

$$\dot{\vec{U}} = \begin{Bmatrix} \dot{U}_x & \dot{U}_y \end{Bmatrix}^T, \left|\dot{\vec{U}}\right| = \sqrt{\dot{U}_x^2 + \dot{U}_y^2} \tag{14}$$

$$\vec{F} = \begin{Bmatrix} F_x & F_y \end{Bmatrix}^T, \left|\vec{F}\right| = \sqrt{F_x^2 + F_y^2} \tag{15}$$

Similarly, Eq. (9) to Eq. (11) can be respectively extended as

$$\vec{F}_1 = \begin{Bmatrix} F_{1x} \\ F_{1y} \end{Bmatrix} = K\vec{U}(t) = a_1\vec{U}(t) + a_2\vec{U}^3(t) + a_3\vec{U}^5(t) \tag{16}$$

$$\dot{\vec{F}}_2 = \left[a_4 + a_5\vec{U}^2(t)\right]\left[\dot{\vec{U}}(t) - \left|\dot{\vec{U}}(t)\right|\left|\frac{\vec{F}_2}{Y_t}\right|^{a_6-1}\right]\frac{\vec{F}_2}{Y_t} \tag{17}$$

$$Y_t = a_7 + \left[1 + \left|\frac{\vec{U}(t)}{a_8}\right|^{a_9}\right] \tag{18}$$

Through mathematically fitting the bilateral test result under one of the test conditions, circular orbit loading with a horizontal shear strain of 200% and a frequency of 0.0125Hz, a set of $a_1 \sim a_9$ in the further extended mathematical model can be identified and are listed in Table 4. To demonstrate the robustness of the

extended model, these determined coefficients are also applied to predict the bilateral hysteresis behavior of HDR bearings under another test condition listed in Table 3. The comparison of the prediction with the test result under circular and figure-eight orbit loading with the same shear strain but a different frequency, 0.1Hz, is shown in Fig.7. The coefficient of determination R^2 is adopted to quantitatively evaluate the difference between the predictions and test results. Apparently, the nine coefficients identified from one test result are also capable of well predicting the bilateral hysteresis behavior of HDR bearings under other test conditions.

Table 4 – Unilateral test protocols under triangular reversal loading

a_1	a_2	a_3	a_4	a_5	a_6	a_7	a_8	a_9
0.12796	-2.5E-06	0.426	0.34770	1.31	1.31921	3.05825	61.3706	2.44623

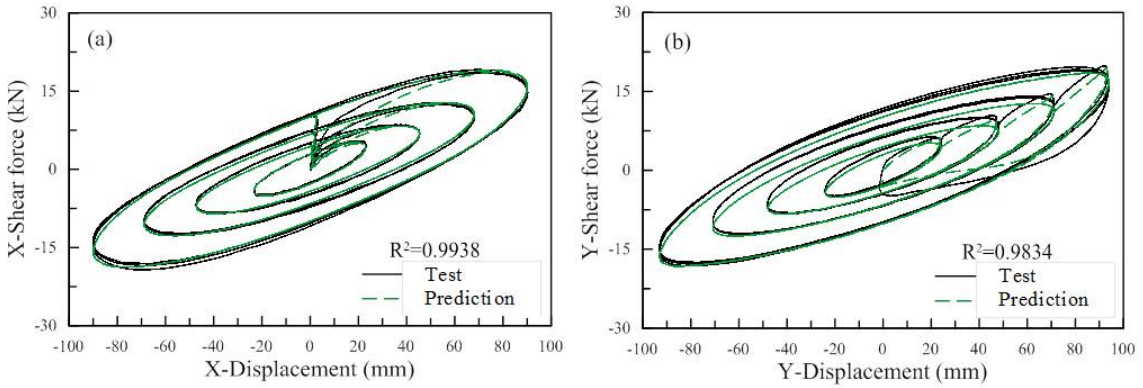

(a) circular orbit (test: 0.1Hz; prediction: 0.0125Hz)

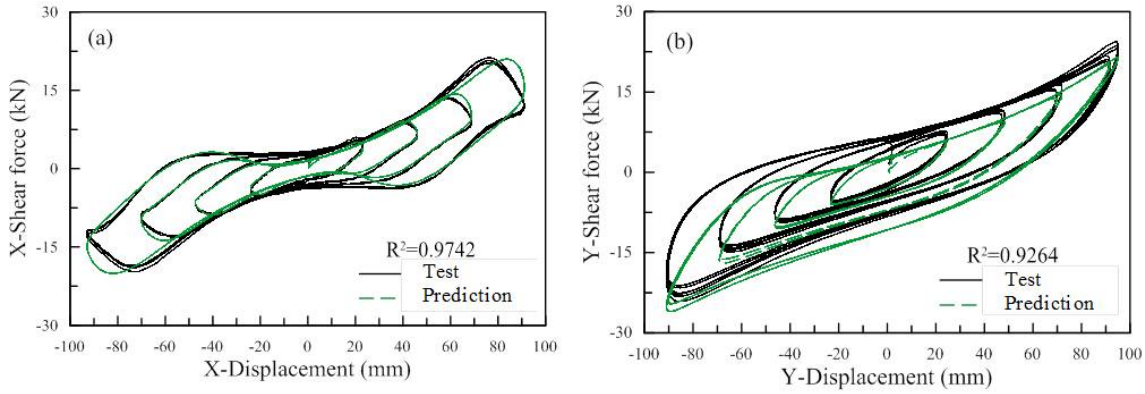

(b) figure-eight orbit (test: 0.1Hz; prediction: 0.0125Hz)

Fig. 7 – Experimental and predicted hysteresis behavior under different bilateral loading patterns (further extended model)

4. Conclusions

In this study, a series of unilateral and bilateral tests are conducted on a scaled-down HDR bearing. Referring to Hwang's and Abe's analytical models, a modified mathematical model which can comprehensively account for the unilateral hysteresis behavior of HDR bearings under sinusoidal and triangular reversal loading is proposed. Besides, a further extended mathematical model is developed for characterizing the bilateral hysteresis behavior of HDR bearings. By comparing the predictions with the test results under circular and figure-eight orbit loading

with different excitation frequency (or velocity) conditions, it can be concluded that the proposed extended mathematical model can well capture the bilateral hysteresis behavior of HDR bearings. The test results also reveal that since the torsional coupling effect results in the local shear strain increased, the effective shear modulus and equivalent damping ratio under non-proportional plane loading become smaller and larger, respectively, compared with those under unilateral reversal loading. It should be carefully taken into account during the design process.

5. References

[1] Hwang JS, Wu JD, Pan TC, Yang G (2002): A mathematical hysteretic model for elastomeric isolation bearing. *Earthquake Engineering and Structural Dynamics*, **31** (4), 771-789.

[2] Abe M, Yoshida J, Fujino Y (2004): Multiaxial behaviors of laminated rubber bearings and their modeling. I: experimental study. *Journal of Structural Engineering*, **130** (8), 1119-1132.

[3] Abe M, Yoshida J, Fujino Y (2004): Multiaxial behaviors of laminated rubber bearings and their modeling. II: modeling. *Journal of Structural Engineering*, **130** (8), 1133-1144.

[4] Özdemir, H. Nonlinear transient dynamic analysis of yielding structures. PhD Dissertation 1973, University of California, Berkeley, Berkeley, Calif.

[5] Yamamoto M, Minewaki S, Yoneda H, Higashino M (2012): Nonlinear behavior of high-damping rubber bearings under horizontal bidirectional loading: full-scale tests and analytical modeling. *Earthquake Engineering and Structural Dynamics*, **41**, 1845-1860.